

Operation of a Triple GEM Detector with CsI Photocathode in Pure CF₄

I. Ravinovich¹, Z. Fraenkel¹, M. Inuzuka², A. Kozlov¹, L. Shekhtman³ and I. Tserruya¹
¹Weizmann Institute of Science, ²University of Tokyo, ³Budker Institute of Nuclear Physics

Abstract—Results obtained with a triple GEM detector operated in pure CF₄ with and without a reflective CsI photocathode are presented. The detector operates in a stable mode at gains up to 10⁴. A deviation from exponential growth starts to develop when the total charge exceeds $\sim 4 \times 10^6$ e leading to gain saturation when the total charge is $\sim 2 \times 10^7$ e and making the structure relatively robust against discharges. No aging effects are observed in the GEM foils after a total accumulated charge of ~ 10 mC/cm² at the anode. The ion back-flow current to the reflective photocathode is comparable to the electron current to the anode. However, no significant degradation of the CsI photocathode is observed for a total ion back-flow charge of ~ 7 mC/cm².

Index Terms—GEM, CsI photocathode, UV-photon detector, CF₄, HBD.

I. INTRODUCTION

WE REPORT on the operation of a triple GEM detector in pure CF₄ with and without a reflective CsI photocathode. This work is part of an R&D program to develop a Hadron Blind Detector (HBD) to upgrade the PHENIX detector at the Relativistic Heavy Ion Collider (RHIC) at BNL [1], [2]. The HBD will allow the measurement of electron-positron pairs from the decay of the light vector mesons, ρ , ω and ϕ and the low-mass pair continuum ($m_{e\bar{e}} \leq 1$ GeV/c²) in Au-Au collisions at energies up to $\sqrt{s_{NN}} = 200$ GeV. The primary choice under study is a windowless Cherenkov detector, operated in pure CF₄ in a special proximity focus configuration, with a reflective CsI photocathode and a triple Gas Electron Multiplier (GEM) [3] detector element with a pad readout.

A. Setup and experimental conditions.

For all the measurements, GEMs produced at CERN were used with 50 μ m kapton thickness, 5 μ m thick copper layers, 60-80 μ m diameter holes and 140 μ m pitch. The GEMs had 3 \times 3 or 10 \times 10 cm² sensitive areas. These two types of GEMs will be referred to in the text as "small" and "large" respectively. Three GEMs were assembled in one stack with G10 frames as shown in Fig. 1. The distance between the GEMs was 1.5 mm and the distance between the bottom GEM (GEM3) and the printed circuit board (PCB) was in most (some) cases 2 mm (1.5 mm). The distance between the top GEM (GEM1) and the drift mesh was 3 mm in the measurements with X-rays and α -particles and 1.5 mm in the measurements with UV-photons.

We use the gap names and the field notations as proposed in [4], i.e. the gap between the mesh and top GEM is called

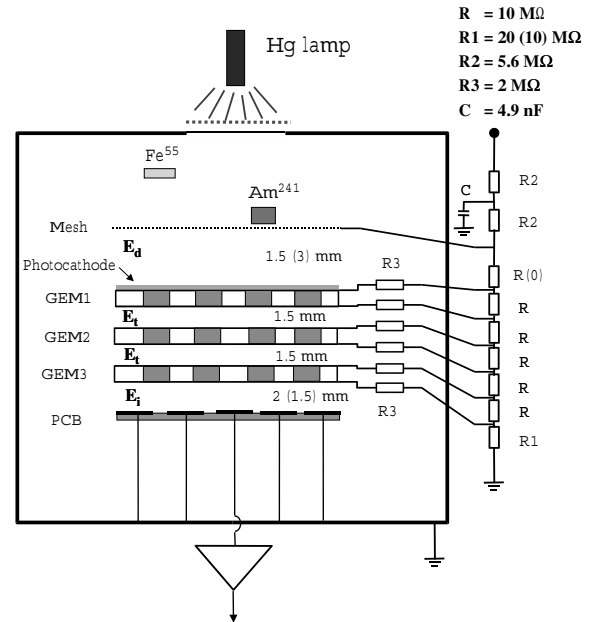


Fig. 1. Setup of the triple GEM detector and resistor chain. The Hg lamp, Fe⁵⁵ and Am²⁴¹ sources were used for measurements with UV-photons, X-rays and α -particles, respectively.

"drift" and the corresponding field is referred to as E_d ; the gaps between GEMs are called "transfer" and the corresponding fields are referred to as E_t ; the gap between GEM3 and the PCB is called "induction" and the corresponding field is referred to as E_i . Most measurements were performed with a 2 mm induction gap and a 20 M Ω resistor feeding it. In this configuration, when the voltage across the GEMs is 510 (370) V, corresponding to a gain of $\sim 10^4$ in CF₄ (Ar/CO₂), the transfer and induction fields are about 3.4 (2.5) kV/cm and 5.1 (3.7) kV/cm, respectively. When R1 is equal to 10 M Ω , the induction fields are half the quoted values. The ability of the GEM to transport electrons through its holes is referred to as "electron transparency". It is the product of two factors: the fraction of electrons collected from the top gap into the holes and the fraction of electrons extracted from the holes into the bottom gap. The electron transparency of the GEMs with the voltages and fields indicated above, can be derived from the data presented in [4]. For GEM1 and GEM2 the electron transparency is close to 1, while for GEM3 it is about 0.7 in

the case of the lower induction field and approaches 1 for the high induction field.

The photocathode was prepared by evaporating a $\sim 2000 \text{ \AA}$ thick layer of CsI on the first GEM previously coated with thin layers of Ni and Au to avoid chemical interaction with the CsI film. For the operation with the reflective photocathode the drift field has to be zero or even reversed in order to collect all the photo-electrons from the CsI layer [5].

The detector assembly (drift mesh, triple-GEM, and PCB) were mounted in a stainless steel box that could be pumped down to 10^{-6} torr and was connected to the inlet and outlet gas lines to allow gas flushing. All measurements were done at atmospheric pressure with an overpressure of 0.5 torr in the detector vessel. The system contained also devices for the precise measurement of temperature, pressure and water content down to the ppm level. The Fe^{55} X-ray source was positioned inside the box at a distance of ~ 40 mm from the mesh. The total rate of X-rays was kept at the level of 1 kHz. 5.9 keV photons from Fe^{55} release 210 e in Ar/CO_2 (26 eV per electron-ion pair) and 110 e in CF_4 (54 eV per electron-ion pair) [7].

B. Gain in Ar/CO_2 and CF_4 .

The gain as a function of the voltage across the GEM (ΔV_{GEM}) was measured with all GEMs at the same voltages for both Ar/CO_2 and pure CF_4 . The absolute gas gain was determined from the measurements of the signal from Fe^{55} 5.9 keV X-ray photons.

The gain was calculated, using the measured relationship between the output signal from the amplifier and the input charge to a calibration capacitor and taking into account the average charge produced by one 5.9 keV photon (see previous section).

Fig. 2 shows the typical gain curves measured with 5.9 keV X-rays in Ar/CO_2 and CF_4 using small and large GEMs. Several detector sets were used and good reproducibility between the various sets was observed. Comparing the data for Ar/CO_2 and CF_4 in Fig. 2 one can see that the operational voltage for CF_4 is ~ 140 V higher but the slopes of the gain-voltage characteristics are similar for both gases, i.e. an increase of 20 V in ΔV_{GEM} causes an increase of the gain by a factor of ~ 3 . The gain in CF_4 can reach values above 10^5 , in spite of the very high operational voltage, as was already reported in [10].

Another feature of CF_4 which can be seen in Fig. 2 is the strong deviation from exponential growth at high gains. This “non-linearity” is much more pronounced when the detector is irradiated with Am^{241} α -particles (Fig. 3). In that figure the saturation level of the pre-amplifier is marked with a dashed line. In the case of Ar/CO_2 the charge depends on ΔV_{GEM} exponentially, and the signal is saturated by the pre-amplifier. In pure CF_4 , on the other hand, the dependence of charge versus ΔV_{GEM} becomes non-linear above the value of $\sim 4 \times 10^6$ e and is completely saturated at $\sim 2 \times 10^7$ e, which is below the saturation level of the pre-amplifier. This difference in performance in Ar/CO_2 and pure CF_4 may be due to the higher

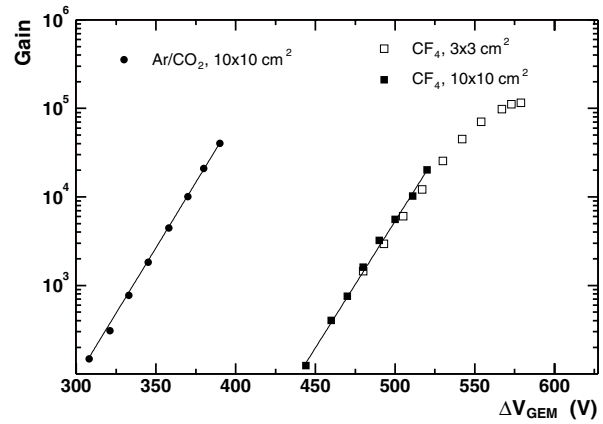


Fig. 2. Gain as a function of GEM voltage measured with Fe^{55} X-ray source. The $3 \times 3 \text{ cm}^2$ detector had a CsI layer deposited on the top face of GEM1. The lines represent exponential fits to the data with $10 \times 10 \text{ cm}^2$ GEMs.

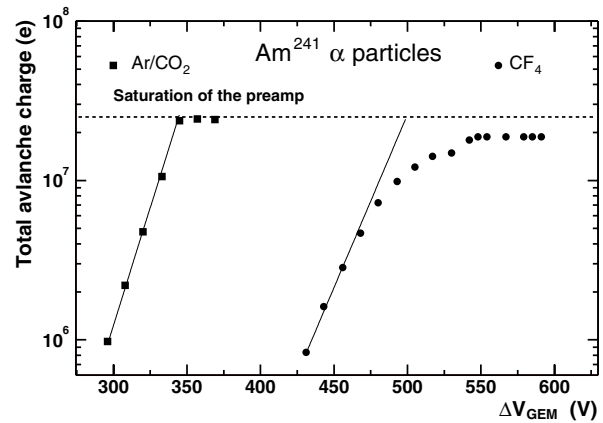


Fig. 3. Total avalanche charge as a function of GEM voltage measured with Am^{241} α -particles. The lines represent exponential growth of the total charge in the avalanche derived from the low gain points

primary charge density and lower diffusion in CF_4 . These two features make the charge cluster in CF_4 more compact and dense and, as a consequence, increase the electric field inside the charge cloud resulting in the saturation of the avalanche. This saturation effect is of prime importance for the anticipated application of the HBD in the PHENIX experiment where single photoelectrons are to be detected in a high multiplicity environment of charged particles.

C. Discharge probability in the presence of heavily ionizing particles.

Stability of operation and absence of discharges in the presence of heavily ionizing particles is crucial for the operation of the HBD. An Am^{241} source was used to simulate heavily ionizing particles under laboratory conditions. We determined quantitatively the probability of discharge as the ratio between the number of discharges within a certain period of time and the number of α -particles traversing the detector during the same

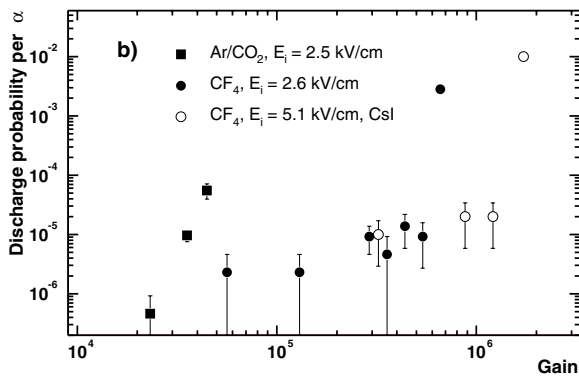
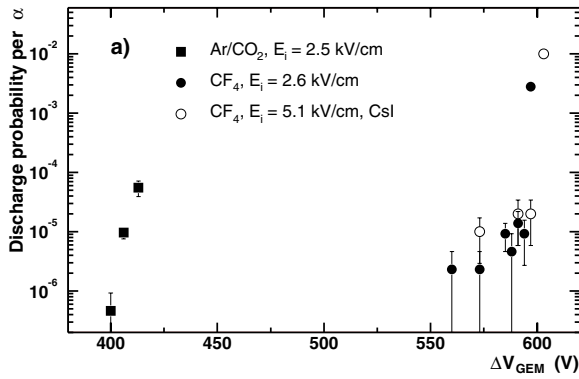


Fig. 4. Discharge probability per α -particle as a function of: a) GEM voltage; b) gain. The values of the induction field E_i refer to a gain of 10^4 . The error bars represent the statistical error. The two highest points for CF_4 represent a lower limit of the discharge probability.

period. The discharge probability was measured in small GEMs and the results are shown in Figs. 4a and 4b in two different forms: as a function of GEM voltage and as a function of gain.

For the Ar/CO_2 mixture the probability of discharge exhibits a rapid increase between 400 V and 420 V across the GEM when the gain reaches 3×10^4 . In terms of gain and GEM voltage these results agree with similar data from [8]. In CF_4 the discharge probability grows at ΔV_{GEM} above 590 V with both $E_i = 2.6$ kV/cm and $E_i = 5.1$ kV/cm. The second setup also had a CsI photocathode on GEM1. From Fig. 3 one can see that the signal from α -particles in CF_4 is completely saturated above $\Delta V_{GEM} \sim 540$ V at the level of $\sim 2 \times 10^7$ e. As a consequence, the total charge produced by the heavily ionizing particle is limited to below the Raether limit [9] and its ability to provoke a discharge is strongly suppressed. Thus, the gain in CF_4 even in the presence of α -particles can reach extremely high values of close to 10^6 . The HBD is expected to operate at gains $\leq 10^4$, i.e. with a comfortable margin below the discharge threshold.

D. Operation with the CsI reflective photocathode.

In all the tests with the CsI photocathode a mercury lamp was used for irradiation. In order to determine the total emission

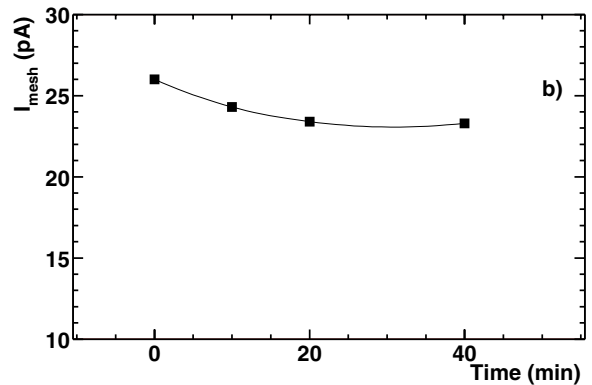
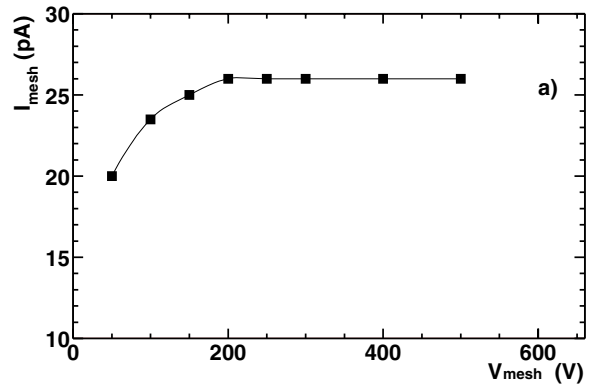


Fig. 5. Current from GEM1 to the mesh: a) as a function of voltage; b) as a function of time. The lines are to guide the eye.

from the photocathode itself without any amplification in the GEMs, we applied a positive voltage between GEM1 and the mesh, thus collecting the emitted photo-electrons in the mesh. The operation of the CsI photocathode is shown in Fig. 5, where the photo-electron current as a function of voltage (5a) and time (5b) is plotted. From Fig. 5a it is seen that in order to measure the full photo-electron emission the voltage between the mesh and GEM1 has to exceed 200 V or, since the drift gap was 1.5 mm, the field has to be higher than 1.3 kV/cm, in agreement with [10].

In Fig. 5b the value of the current to the mesh as a function of time is shown, demonstrating that one has to wait about 30 min after the application of the HV in order to stabilize the signal. As CsI is a semi-insulating material, this initial instability of the signal might be caused by polarization and up-charging of the layer.

The study of the triple GEM detector with a reflective photocathode was always performed in the regime with $E_d = 0$. Fig. 6 shows the current to the PCB as a function of the GEM voltage for the small GEM setup. The measurements were done in Ar/CO_2 and CF_4 . In the CF_4 curve we can clearly see two regions well described by two exponential dependencies on ΔV_{GEM} (see lines in Fig. 6): an initial slow increase of current at lower voltages related to the increase of the extraction of the photo-electrons from the CsI surface into the holes of

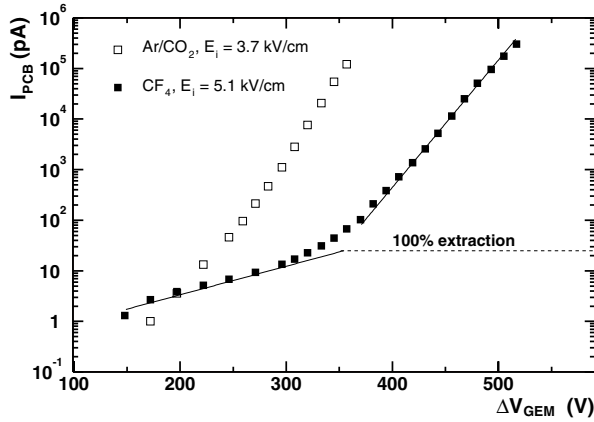


Fig. 6. Current to the PCB as a function of ΔV_{GEM} .

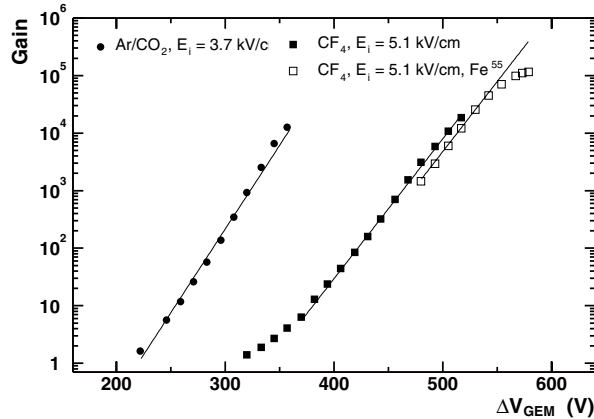


Fig. 7. Gain as a function of ΔV_{GEM} for Ar/CO₂ and CF₄ measured with the UV lamp. For CF₄, the gain curve with Fe⁵⁵ is also shown. The lines are exponential fits to the data.

GEM1 and a steep exponential increase at higher voltages due to amplification in the GEMs. A detailed discussion of these processes and the transition from one region to the other can be found in [11]. In Ar/CO₂ these two regions are not so clearly separated because amplification in this mixture starts at lower voltages. The electron extraction cannot exceed the maximum level shown in Fig. 5a. It indeed seems to reach this level of 100% extraction indicated by the dashed line in Fig. 6. Thus, the gain is determined as the ratio between the current to the PCB and the extraction current. The latter is given by the first exponential curve up to $\Delta V_{GEM} = 350$ V and by the 100% extraction value at higher values of ΔV_{GEM} .

The gain as a function of ΔV_{GEM} for the setup with the reflective photocathode is shown in Fig. 7. In the same figure the data obtained with X-ray irradiation (Fe⁵⁵) are also shown in order to demonstrate that the different methods of gain measurement give similar results.

E. Ion back-flow in the triple GEM detector operating with a reflective photocathode.

The flow of positive ions to the CsI layer is one of the potential damaging factors that can cause aging of the photocathode [6], [12], [13], [14]. We call this factor ion back-flow and characterize it by the ratio between the current to the top electrode of GEM1 and the current to the PCB. This ratio depends on both the ion current itself and the fraction of electron current flowing to the PCB. This is a convenient definition as it allows us to estimate the actual ion current from the measured signal at the PCB.

In Fig. 8 the ratio of the current to the photocathode and the current to the PCB (ion back-flow factor) as a function of gain is shown for different conditions. The errors on the plots are mainly due to the limited accuracy of the photocathode current measurements. The value of the induction field was changed by changing the corresponding resistor in the chain and the value, indicated in the caption (5.1 kV/cm), is reached at a gain of 10^4 .

In Fig. 8a we see that in spite of the very different transport properties of the gases used in the measurements no significant dependence of the ion back-flow factor on the nature of the gas is observed as a function of gain and for different induction fields. The insensitivity of the ion back-flow factor to the particular gas at moderate gains is similar to that seen in [13]. It means that the efficiency of the transport of electrons and ions through the GEMs is the same for both gases and does not depend on diffusion.

The insensitivity of the ion back-flow factor to the electric field between the GEMs and in the GEM is demonstrated in Fig. 8b. Here the value of the ion back-flow factor as a function of gain is shown for three different electrostatic conditions: 1) standard, when the transfer field is equal to 3.4 kV/cm for both gaps and the induction field is equal to 5.1 kV/cm (the values refer to a gain of 10^4), 2) enhanced transfer field in both gaps, 3) reduced field in GEM1. From Fig. 8b we see that neither variation in electrostatic conditions between nor inside the GEMs affect significantly the ion back-flow factor.

The only parameter which affects the value of the ion back-flow in our case is the induction field. Fig. 8c shows the value of the ion back-flow factor as a function of the gain for 3 values of the induction field. The field in the induction gap does not affect the ion flow itself as ions are produced in the holes of the last GEM or in their vicinity, collected into the holes and then transported to the top gap. The only factor that is affected is the electron flow from GEM3 to the PCB. Thus the ion back-flow factor being higher than one at low induction field means that a fraction of the electrons is collected at the bottom face of GEM3 and consequently the amount of ions reaching the photocathode can be larger than the amount of electrons collected at the PCB. The increase of the induction field improves the electron collection efficiency at the PCB and reduces the value of the ion back-flow factor. It is clear from the figure that for E_i above 5 kV/cm the collection efficiency does not increase significantly resulting in a minimum value of

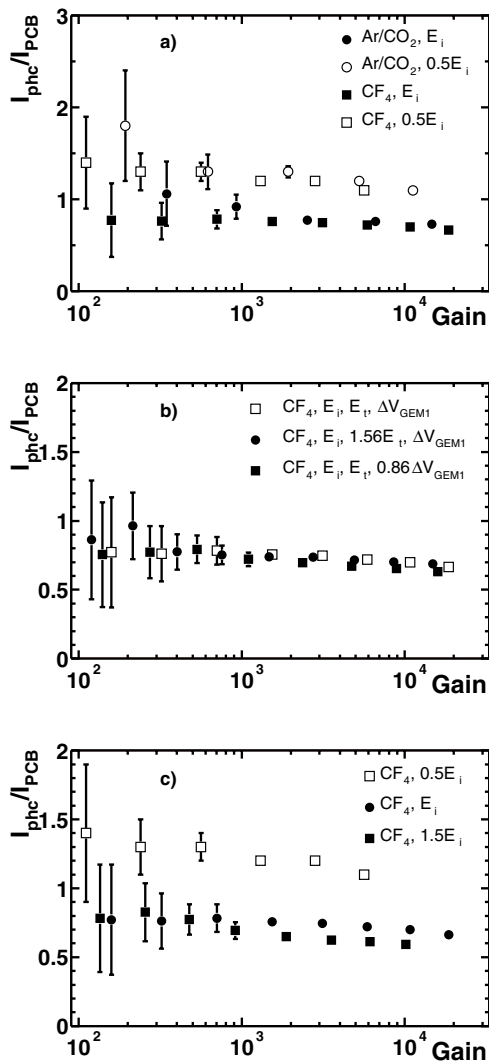


Fig. 8. Ion back-flow factor as a function of gain. a) Comparison of ion back-flow factor for Ar/CO₂ and CF₄ and two different induction fields: standard $E_i = 5.1$ kV/cm and $0.5 E_i$. The values refer to a gain of 10^4 ; b) Ion back-flow factor for different electrostatic conditions in the region between GEM1 and GEM3. c) Ion back-flow factor for 3 different values of the induction field.

the ion back-flow factor of ~ 0.7 at a gain of 10^4 , consistent with results of [12].

During these measurements the photocathode was exposed to a total ion charge of ~ 7 mC/cm². This charge density corresponds to ~ 10 hours of continuous irradiation with $\sim 10^7$ photons/(mm²×s) at a gain of 10^4 . In spite of this quite high ion back-flow the CsI quantum efficiency loss was not more than 30% after this irradiation.

II. CONCLUSION

We have presented very encouraging results on the operation of a triple GEM detector in pure CF₄ with and without a reflective CsI photocathode. The slope of the gain curve

is similar to that of the conventional Ar/CO₂ (70/30%) gas mixture, however ~ 140 V higher voltage across the GEMs is needed for a given gain. The gain curve starts deviating from exponential growth when the total charge in the detector exceeds $\sim 4 \times 10^6$ e, and the gain is fully saturated when the total avalanche charge reaches $\sim 2 \times 10^7$ e. This is an interesting property making the system more robust against discharges as compared to Ar/CO₂. Stable operation can be achieved at gains up to 10^4 in the presence of heavily ionizing particles. No deterioration of the GEM foil performance in a pure CF₄ atmosphere was observed for a total accumulated charge of ~ 10 mC/cm² at the PCB. The ion back-flow to the photocathode is close to 100%, independent of the operating gas and of the transfer field E_t between successive GEMs. At a gain of 10^4 , the ion back-flow factor can be reduced to $\sim 70\%$ by applying a relatively high induction field of $E_i \sim 5$ kV/cm. In spite of the high ion back-flow no sizable deterioration of the CsI quantum efficiency was observed when the photocathode was exposed to a total ion charge of ~ 7 mC/cm². This value is larger by about two orders of magnitude than the total integrated ion charge density expected during the lifetime of the planned HBD.

ACKNOWLEDGMENT

We thank F. Sauli, A. Breskin, R. Chechik, M. Klin and D. Mörmann for their invaluable help and very useful discussions. This work was partially supported by the Israel Science Foundation, the Nella and Leon Benoziyo Center of High Energy Physics Research and the US Department of Energy under Contract No. DE-AC02-98CH10886.

REFERENCES

- [1] A. Kozlov, I. Ravinovich, L. Shekhtman, Z. Fraenkel, M. Inuzuka and I. Tseruya, submitted to Nucl. Instr. and Meth..
- [2] Z. Fraenkel, B. Khachaturov, A. Kozlov, A. Milov, D. Mukhopadhyay, D. Pal, I. Ravinovich, I. Tseruya and S. Zhou, PHENIX Technical Note 391. <http://www.phenix.bnl.gov/phenix/WWW/forms/info/view.html>, 2001.
- [3] F. Sauli, Nucl. Instr. and Meth. A386 (1997), 531.
- [4] S. Bachmann, A. Bressan, L. Ropelewski, F. Sauli, A. Sharma, D. Mörmann, Nucl. Instr. and Meth. A438 (1999), 376.
- [5] D. Mörmann, A. Breskin, R. Chechik, P. Cwetanski and B. K. Singh Nucl. Instr. and Meth. A478 (2002), 230.
- [6] B. K. Singh, E. Shefer, A. Breskin, R. Chechik and N. Avraham, Nucl. Instr. and Meth. A454 (2000), 364.
- [7] Archana Sharma, <http://consult.cern.ch/writeup/garfield/examples/gas/trans2000.html>.
- [8] S. Bachmann et al., Nucl. Instr. and Meth. A479 (2002), 294.
- [9] H. Raether, Z. Phys. 112 (1939), 464.
- [10] A. Breskin, A. Buzulutskov and R. Chechik, Nucl. Instr. and Meth. A483 (2002), 670.
- [11] C. Richter, A. Breskin, R. Chechik, D. Mörmann, G. Garty and A. Sharma, Nucl. Instr. and Meth. A478 (2002), 538.
- [12] D. Mörmann, A. Breskin, R. Chechik and D. Bloch, submitted to Nucl. Instr. and Meth. (in press).
- [13] A. Bondar, A. Buzulutskov, L. Shekhtman and A. Vasiljev, Nucl. Instr. and Meth. A496 (2003), 325.
- [14] F. Sauli, S. Kappler and L. Ropelewski, IEEE Nuclear Science Symposium (Norfolk, November 12-14, 2002) to be published.